Photodisintegration of U^{235}

C. D. Bowman, G. F. Auchampaugh, and S. C. Fultz
Lawrence Radiation Laboratory, University of California, Livermore, California
(Received 27 September 1963)

The photodisintegration of U^{235} has been studied, using nearly monochromatic photons obtained from the annihilation in flight of fast positrons. The partial cross sections $\sigma(\gamma,F)$, $\sigma(\gamma,n)$, and $\sigma(\gamma,2n)$ were determined. Integrated cross sections for these reactions were found to be 1.07, 1.00, and 1.49 MeV·b, respectively. Structure in the giant resonance of the compound-nucleus-formation cross section was observed and from this a quadrupole moment of 12.8±1.3 b was found. An energy dependence in the quantity Γ_n/Γ_f was observed.

INTRODUCTION

THE cross sections for photon-induced neutron emission and fission have been investigated in a wide range of heavy nuclei, mainly with bremsstrahlung radiation[1–4] or photons from the $F^{19}(p,\alpha\gamma)O^{16}$ reaction.[5] However, the accuracy of these measurements was somewhat limited, in the former case by the difficulty of analyzing bremsstrahlung data, and in the latter by the low intensity of the photon source and the limited variability of the photon energy. Using such methods it has not been possible, therefore, to investigate many aspects of the processes which are of interest. For instance, it is well-known that the fissionable nuclei are highly deformed.[6] According to Danos[7] and Okamoto,[8] a splitting is to be expected in the giant-dipole resonance of the compound-nucleus-formation cross section. Although such a splitting has been observed in the rare-earth nuclei by several investigators,[9,10] it has not been detected in the fissionable elements.

The measurement of the nuclear-formation cross section is complicated by the competition of fission with neutron emission.[3] This competition is usually expressed in terms of the ratio of the probabilities for neutron emission relative to fission, i.e., Γ_n/Γ_f. At present, there is considerable experimental evidence that this ratio does not depend strongly on the excitation energy of the compound nucleus. Fission and neutron emission induced by moderate energy neutrons, charged particles, and bremsstrahlung are explained satisfactorily on the basis of an energy-independent value for Γ_n/Γ_f.[11–13] The data on nuclear excitation by photons are, however, not sufficiently accurate for such a dependence to be observable, due to the averaging inherent in the bremsstrahlung process.

The Bohr model for fission[14] implies that the fissionability of the nucleus might be strongly dependent on the angular momentum and parity of the excited nucleus. Since the particle-induced spallation and fission experiments were carried out at an energy for which a wide variety of angular momentum and either parity are possible, these quantum numbers would place little restriction on the fission process. However, for moderate-energy photons, the angular momentum and the parity of the compound nucleus are much more restricted, since only magnetic- and electric-dipole or electric-quadrupole interactions usually occur. Therefore, the charged-particle results do not preclude the possibility of an energy dependence in Γ_n/Γ_f when the nucleus is excited by moderate-energy photons.

The possibility of the variation of Γ_n/Γ_f and its effect on the measurement of the splitting of the giant-dipole resonance in U^{235} have been studied in the work reported here. For these measurements, monoenergetic photons produced by the annihilation in flight of positrons were used. Three measurements were performed under identical photon-resolution conditions: (1) The fission cross section was determined. (2) The cross sections for neutron emission were determined. (3) The average multiplicity of neutrons per photon interaction with the nucleus was measured. These data in combination with the known information on the energy dependence of $\bar{\nu}$,[15] the average number of neutrons emitted per fission, have been analyzed for the (γ,n) and $(\gamma,2n)$ cross sections and the shape of the giant dipole resonance. A splitting in the giant dipole

[1] G. C. Baldwin and G. S. Klaiber, Phys. Rev. **71**, 3 (1947).
[2] J. Gindler, J. Huizenga, and R. Schmitt, Phys. Rev. **104**, 425 (1956).
[3] L. Katz, A. P. Boerg, and F. Brown, in *Proceedings of the Second International Conference on the Peaceful Uses of Atomic Energy, Geneva, 1958* (United Nations, Geneva, 1958), Vol. 15, p. 200.
[4] E. J. Winhold and I. Halpern, Phys. Rev. **103**, 990 (1956).
[5] R. O. Haxby, W. E. Shoupp, W. E. Stephens, and W. A. Wells, Phys. Rev. **59**, 57 (1941).
[6] A. Bohr and B. R. Mottelson, Kgl. Danske Videnskab. Selskab, Mat. Fys. Medd. **27**, No. 16 (1953).
[7] M. Danos, Nucl. Phys. **5**, 23 (1958).
[8] K. Okamoto, Progr. Theoret. Phys. (Kyoto) **15**, 75 (1956).
[9] E. G. Fuller and M. S. Weiss, Phys. Rev. **112**, 560 (1958).
[10] R. L. Bramblett, J. T. Caldwell, G. F. Auchampaugh, and S. C. Fultz, Phys. Rev. **129**, 2723 (1963).
[11] R. Vandenbosch and G. T. Seaborg, Phys. Rev. **110**, 507 (1958).
[12] R. Vandenbosch, T. D. Thomas, and S. E. Vandenbosch, Phys. Rev. **111**, 1358 (1958).
[13] R. A. Glass, R. J. Carr, J. W. Cobble, and G. T. Seaborg, Phys. Rev. **104**, 434 (1956).
[14] A. Bohr, in *Proceedings of the International Conference on the Peaceful Uses of Atomic Energy, Geneva, 1955* (United Nations, New York, 1956), Vol. 2, p. 151.
[15] J. C. Hopkins and B. C. Diven, Bull. Am. Phys. Soc. **8**, 121 (1963).

resonance was observed and the sign and magnitude of the associated intrinsic nuclear-quadrupole moment was determined.

PHOTOFISSION MEASUREMENTS

A multiple-plate ionization chamber was used, containing 12.71 g of uranium enriched to 93% in U^{235}. The uranium was deposited on aluminum plates to a thickness of 0.5 mg/cm^2. Since absolute cross sections for the photofission process were desired, the chamber efficiency was required. This was obtained by placing the chamber in a slow-neutron flux of known intensity and energy. Using the energy dependence of the epithermal-neutron-fission cross section[16] for U^{235}, the chamber efficiency was then determined. Isotropy of the fission-fragment angular distribution for both photon- and slow-neutron-induced fission of U^{235} is expected on theoretical grounds[14] and has been confirmed by experiment.[3,4,17] Angular distribution effects, therefore, did not affect the efficiency determination. Corrections due to the different attenuations of the photon or neutron beams traversing the chamber were negligible.

The photofission measurements were performed with the chamber placed in the photon-monochromator arrangement as shown in Fig. 1. Positrons and electrons were accelerated by the Livermore 26-MeV linear electron accelerator in pulses of 2-μsec duration at a repetition rate of 200 pps. Monoenergetic photons of variable energy were produced by annihilation in flight of the positrons in a thin lithium hydride (LiH) target. The effect of the bremsstrahlung photons, which also resulted from the positron interaction in LiH, was determined by similar measurements performed with the electrons. The combined effect of the energy spread of the beam, the LiH-target thickness, and the photon collimation gave an energy resolution of annihilation photons of 3% or better. The photon beam was monitored by a calibrated xenon-filled ionization chamber placed between the LiH target and fission chamber. Pulses from the fission chamber were monitored in a 3-μsec interval bracketing the 2-μsec photon burst. A smooth curve was drawn through the bremsstrahlung data. The dots of Fig. 2 represent the difference between the positron and electron measurements. The error bars represent the standard deviation in the number of fissions detected in the positron measurements. More details on the photon monochromator and the analytical procedure to obtain the cross section are given elsewhere.[18]

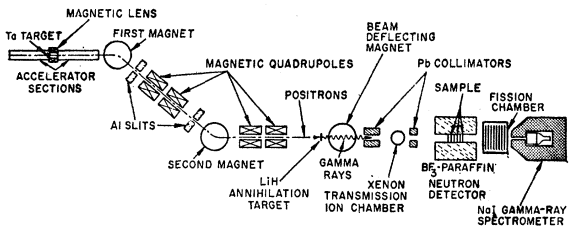

FIG. 1. Experimental apparatus for the photodisintegration measurements (not to scale). For the photofission measurements, the fission chamber was placed between the neutron detector and the gamma-ray spectrometer. The spark chamber was at the same position with the calibrated ionization chamber immediately behind the neutron detector. Neutron- and gamma-ray shielding has been omitted.

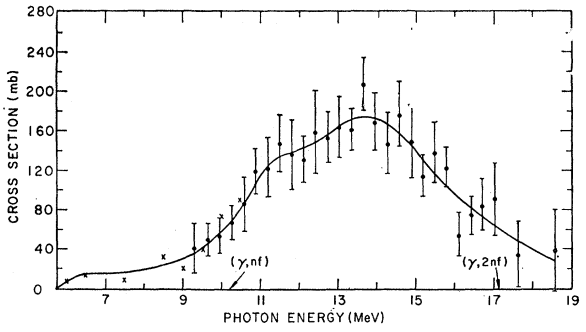

FIG. 2. Photofission cross section $\sigma(\gamma,F)$ of U^{235}. The data denoted by dots represent the fission cross section as measured with the annihilation photons. Error bars give standard deviation in the positron data. The crosses represent normalized bremsstrahlung data obtained with the spark chamber. The solid line through the data represents the photofission cross section used in the analysis for the formation cross section.

In the photofission experiments performed with electron bremsstrahlung at other laboratories, it was necessary to use a compensated ionization-fission chamber to observe the fission fragments above the pulse of ionization produced by the photon burst.[1] However, for the present annihilation-photon experiment, the photon intensities were sufficiently small that no such compensation was required. For such low photon intensities, it was necessary to take precautions to eliminate several sources of background. By proper adjustment of the bias level, the background due to the pileup of the natural alpha-particle activity of the U^{235} and that due to spurious electronic effects were reduced to a level of about 1 pph. The most troublesome source of backgrou id was that caused by slow- or fast-neutron-induced fission. These neutrons could originate near the accelerator or in the vicinity of the LiH target and the photon-collimation system. The chamber was shielded from the fast neutrons originating at the accelerator by a 3-ft-thick concrete wall between the accelerator and the experimental area. By surrounding the chamber with a 6-in. layer of compressed boracic acid, the chamber was further protected from the extraneous neutron field in the experimental area. The remaining possible sources and neutrons which might

[16] C. D. Bowman, G. F. Auchampaugh, and S. C. Fultz, Phys. Rev. **130**, 1482 (1963).

[17] J. E. Brolley, Jr., and W. C. Dickenson, Phys. Rev. **94**, 640 (1954).

[18] S. C. Fultz, R. L. Bramblett, J. T. Caldwell, and N. A. Kerr, Phys. Rev. **127**, 1273 (1962).

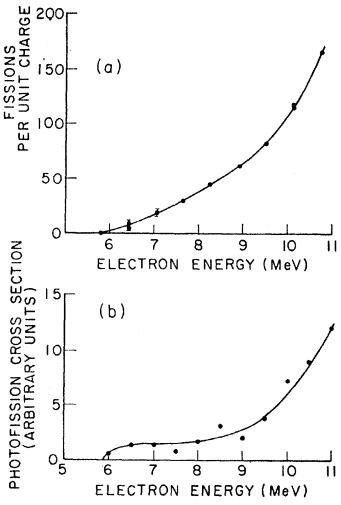

FIG. 3. Bremsstrahlung data on the photofission cross section of U^{235}. (a) Relative bremsstrahlung-yield curve obtained with the spark chamber, expressed in fissions per unit charge. The standard deviation in the data is less than the size of the dots, except when noted otherwise. (b) Photofission cross section in arbitrary units, obtained by unfolding the bremsstrahlung data.

influence the measurements were the LiH target and the photon collimator. The fast-neutron flux from these sources was found to be negligible as compared to the photon flux. Since the fission cross sections for fast neutrons and for photons are roughly of the same order of magnitude, the effect of fast neutrons is negligible. Any slow neutrons, which would induce fission with very high probability, are gated out by time of flight since the detector is gated on only for 3 μsec around the beam burst.

The background from all sources was found to be about 4 pph. This is about 5% of the counting rate at the peak of the giant resonance. As described earlier, the procedure for deducing the cross section from the experimental data required a subtraction of the neutron measurements made with electrons from those made with positrons. Background effects are therefore mostly cancelled out. The small background which remained in the data after this subtraction was, therefore, neglected.

Since the photon yield from the monochromator decreases rapidly with energy below 10 MeV, the experiments with the fission chamber were impossible below 9 MeV. To fill in the gap from 9 MeV down to fission threshold, an attempt was made to use bremsstrahlung from the much more intense electron beam which is available when the accelerator is operated without the restrictions imposed by the photon-monochromator arrangement. However, under these conditions, the ionization induced by photons traversing the chamber exceeded that due to the fission fragments. A corona-type spark chamber, which has the advantage of being very insensitive to gamma rays, was therefore used as a fission-fragment detector in the measurements below 9 MeV. Such a detector is ideally suited to this type of experiment since, in addition to its insensitivity to photons, it can be made to detect fission fragments with an efficiency as high as 30% while discriminating effectively against the alpha-particle background of the fissionable material.[19]

A 2-in.-square aluminum plate covered on one side with $\frac{1}{2}$ mg/cm^2 of U^{235} was used as the fission sample in these experiments. The side of the plate covered with U^{235} was placed $\frac{1}{8}$ in. above the sensitive area of the spark chamber. The sample and detector were placed in a collimated beam of bremsstrahlung photons produced by the interaction of the electron beam from the accelerator with a 0.003-in.-thick tantalum target, which was substituted for the LiH target. The photon beam was monitored by means of a calibrated transmission-ionization chamber[20] placed between the neutron detector shown in Fig. 1 and the spark chamber. This ionization chamber was used to measure the integrated total γ-ray energy (γ-MeV) incident upon the spark chamber during each measurement. The number of fissions induced in U^{235} per arbitrary unit of integrated photon energy (accumulated charge) as a function of electron energy is given in Fig. 3(a). The yield curve was unfolded from the bremsstrahlung spectrum, using the Penfold and Leiss[21] procedure. After drawing a smooth curve through the points, values were taken from the curve every 0.5 MeV in accordance with the tabulation of Penfold and Leiss. The results are given in Fig. 3(b). The threshold and onset of the giant dipole resonance are clearly visible. The cross-section scale was then obtained by matching the bremsstrahlung (spark chamber) results with the annihilation-photon (ion chamber) measurements in the overlap region of 9 to 11 MeV.

The combined results of the two photofission measurements are given in Fig. 2 where the ordinate is defined as

$$\sigma(\gamma,F)=\sigma(\gamma,f)+\sigma(\gamma,nf)+\sigma(\gamma,2nf)+\cdots \quad (1)$$

following the terminology introduced by Gindler, Huizenga, and Schmitt.[2] The dots represent the annihilation photon data and the crosses represent the normalized spark-chamber data. Although the data are somewhat sparse, some structure in the photofission cross section is apparent. The solid curve drawn through the data represents the cross section used in the analysis and interpretation of the experiments.

PHOTONEUTRON MEASUREMENTS

The neutron detector for the photoneutron measurements consisted of 24 BF_3 proportional counters embedded in an 18-in. cube of paraffin. The photon beam passed down the axis of the cube through a 3-in.-diam hole. A 147-g sample of metallic U^{235} enriched to 93% was used for the photoneutron measurements. The

[19] C. D. Bowman and R. W. Hill, Nucl. Instr. Methods **24**, 213 (1963).
[20] E. G. Fuller and Evans Hayward, J. Res. Natl. Bur. Std. U. S. **65A**, 401 (1961).
[21] A. S. Penfold and J. E. Leiss, Univ. Illinois, R. Phys. Res. Lab. Rept., 1958 (unpublished).

$2\frac{1}{4}$-in.-diam cylindrical sample was placed with its flat faces perpendicular to the axis of the hole and at the center of the cube. To prevent neutron regeneration in the U^{235} by slow-neutron fission, the sample was covered on its circumference by a $\frac{1}{32}$-in.-thick layer of Cd and on its two flat faces by a $\frac{1}{8}$-in.-thick layer of a mixture composed of equal weights of B^{10} and paraffin.

Signals from the neutron detector were recorded during a 440-μsec gating interval. The effects of the photon burst and accelerator pickup were eliminated by delaying the start of this gate by 7 μsec with respect to the 2-μsec beam burst. The efficiency of the detector with this gating arrangement and with the U^{235} sample in position was determined by use of neutrons from the spontaneous fission of Cf^{252}. The average number of neutrons emitted per spontaneous fission has been recently well-established at 3.77.[15,22] The Cf^{252} source was placed at the center of the neutron detector. The pulse from a solid-state detector which was used to detect the spontaneous fission fragments gated the detector on after a 7-μsec delay. The source was weak enough so that the overlap of neutrons from one fission to the next was negligible. For a given efficiency measurement, the number of gating pulses and the total number of neutrons detected during these gates were measured. The average number of neutrons detected per fission when divided by the actual number omitted per fission gives the efficiency. This procedure yielded an efficiency of 17.6±0.2%.

A complete knowledge of the various cross sections requires a measurement of the total neutron-emission cross section, denoted as $\sigma(\gamma,N)$, as a function of energy as well as a measurement of the multiplicity of neutron emission. The expression $\sigma(\gamma,N)$ can be written

$$\sigma(\gamma,N)=\sigma(\gamma,n)+2\sigma(\gamma,2n)+3\sigma(\gamma,3n)+\cdots+\bar{\nu}\sigma(\gamma,F), \quad (2)$$

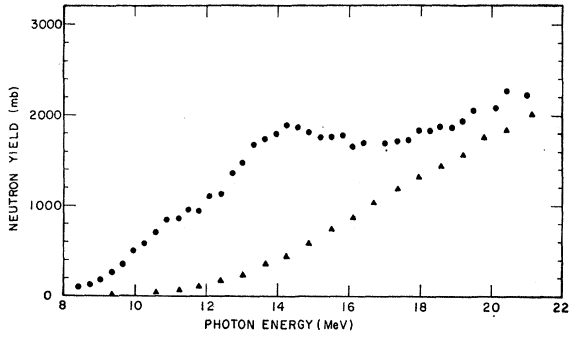

FIG. 4. Neutron yield from positrons and electrons. Upper curve gives neutron yield as a function of photon energy obtained by measurements with positrons. The same quantity obtained with electrons is given in the lower curve. These measurements were normalized to equal numbers of positrons and electrons. Sample-out corrections to the data have been included.

[22] I. Asplund-Nillson, H. Conde, and N. Starfelt, Nucl. Sci. Eng. 16, 124 (1963).

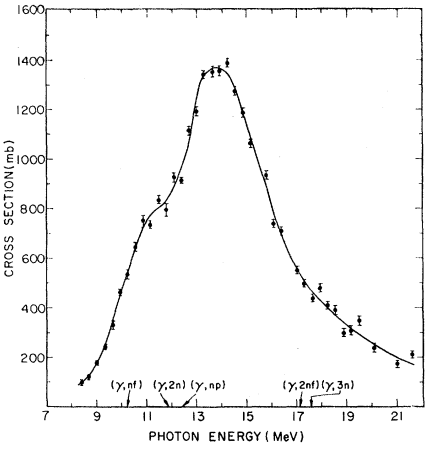

FIG. 5. Total neutron-emission cross section $\sigma(\gamma,N)$ for U^{235}. These data were obtained by taking the difference between the neutron-yield curves of Fig. 4. The statistical errors on the points represent the standard deviation of the measurements with positrons. The thresholds for various reactions which emit neutrons are also shown.

where $\sigma(\gamma,F)$ is the cross section for fission and $\bar{\nu}$ is the average number of neutrons emitted per fission. The neutron yield as a function of positron and electron energy was determined in the usual way,[18] from 9 to 21 MeV, using the xenon-ionization chamber as the photon-flux monitor. The U^{235} disk was then removed from the sample holder leaving the Cd and B^{10} slow-neutron filters in the photon beam. The measurements were repeated and the resulting neutron yield was subtracted from the first measurement to give the neutron yield arising from only the U^{235}. The magnitude of this sample-out correction was about 5%. The measurements taken with positrons and electrons corrected in this way and normalized to equal number of positrons and electrons are shown in Fig. 4. A smooth line was drawn through the electron data and the difference between the two curves taken to give the $\sigma(\gamma,N)$ cross section of Fig. 5.

The last experiment required to determine uniquely the compound-nucleus-formation cross section was the measurement of the multiplicity of neutron emission. The multiplicity can be expressed in terms of a quantity μ defined as the average number of neutrons emitted per formation of the compound nucleus. If the formation cross section $\sigma(\gamma,\text{total})$ is defined as

$$\sigma(\gamma,\text{total})=\sigma(\gamma,n)+\sigma(\gamma,2n)+\cdots+\sigma(\gamma,f)+\sigma(\gamma,nf)+\sigma(\gamma,2nf)+\cdots, \quad (3)$$

then μ is given as

$$\mu=\sigma(\gamma,N)/\sigma(\gamma,\text{total}). \quad (4)$$

This quantity was determined between 7 and 23 MeV by measuring the multiplicity of neutrons detected per beam burst. An electronic-sorting circuit was employed to determine whether one, two, or up to six neutrons were detected in a beam burst. The measured quantities

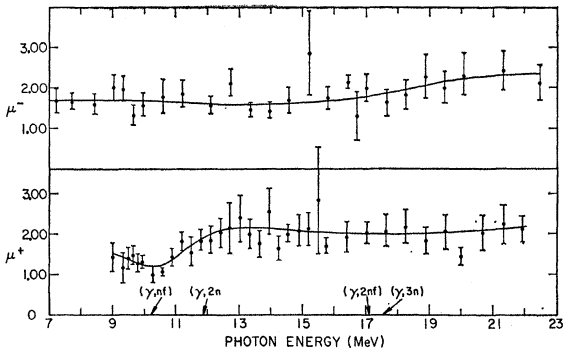

FIG. 6. Energy dependence of the quantities μ^+ and μ^-. The error bars represent the standard deviation computed from the propagation of the statistical error in P_N through Eq. (10).

are related to the multiplicity of neutron emission in a rather complex manner due to the possibility of more than one photon interaction per beam burst and a neutron detection efficiency of less than 100%. A proper analysis of the data requires that the photon intensity per beam burst be constant throughout a measurement at some particular energy. Since the photon intensity has a long-period drift in addition to a considerable pulse-to-pulse variation, it was important that only those photon bursts within a rather limited variation in intensity be accepted for analysis by the sorting electronics. The relative beam intensity was therefore monitored so that only those accelerator pulses whose intensity varied less than $\pm 10\%$ from the mean intensity were analyzed. This pulse was then used to gate the two sorting circuits used for the multiplicity analysis. The xenon ionization chamber, which ordinarily monitored the photon flux, was not used since it could not be gated due to the manner of charge collection and measurement. However, as will be shown later, the photon flux is not necessary to a determination of μ if $\sigma(\gamma,N)$ is known. Corrections to the observed multiplicity due to analyzer dead time were applied. Since the electronic dead time of 1.5 μsec was small as compared to the 137.5-μsec decay constant of the neutron detector, these corrections were usually negligible as compared to statistical uncertainty in the multiplicity measurements.

The parameter μ defined by Eq. (4) is actually not the quantity that is measured by the procedure outlined above. The measured quantity is the weighted average of μ over the photon spectrum produced in either the positron or electron runs and is denoted by μ^+ and μ^-, respectively. When μ^+ and μ^- are combined with a knowledge of the ratio of the number of neutrons released for equal numbers of positrons and electrons as determined in the $\sigma(\gamma,N)$ experiment, these data can be used to determine μ.

ANALYSIS

The quantities $\mu^\pm$ can be obtained from experimental multiplicity data. To review the experimental procedure briefly, bursts of gamma rays strike a sample and induce neutron-emitting reactions. The neutrons are detected with an efficiency ϵ. Although the probability of inducing at least one neutron-releasing interaction per beam burst is very small (~ 0.01), it is still necessary to take into account the possibility of more than one such reaction taking place. The problem then is to find the probability p_l that a gamma ray in traversing the U-235 sample will induce a reaction emitting l neutrons. The probability that a photon will interact with the nuclei in the sample is then given by

$$\sum_{l=1}^{\infty} p_l.$$

Let P_N be the measured multiplicity, i.e., the probability that N neutrons will be detected per beam burst when the average number of photons per beam burst is a. The relation between the P_N and p_l has been derived by determining the relationship between the generating function for these two probabilities. The generating function $G(r)$ for the p_l is defined as

$$G(r)=\sum_{l=0}^{\infty} p_l r^l. \tag{5}$$

If $G(r)$ can be determined, then p_l can be obtained according to the definition by means of the expression

$$p_l=(1/l!)[\delta G(r)/\delta r^l]|_{r=0}. \tag{6}$$

A similar expression $G(s)$ can be written for the P_N. The relationship between these two generating functions has been found[23] to be

$$G(s)=\exp\{a[G(r)-1]\}, \tag{7}$$

where $r=(1-\epsilon+\epsilon s)$. This can be rewritten explicitly in terms of the p_l and P_N as

$$G(r)=\sum_{l=0}^{\infty} p_l r^l=1+\frac{1}{a}\ln\sum_{N=0}^{\infty} P_N s^N. \tag{8}$$

The p_l can be determined from this relation by performing the operation indicated in Eq. (6). The quantities $\mu^\pm$ can then be obtained from Eq. (8) using an alternative definition for μ,

$$\mu^\pm=\sum_{l=1}^{\infty} l p_l^\pm \Big/ \sum_{l=1}^{\infty} p_l^\pm, \tag{9}$$

where the superscript sign on p_l denotes positrons or electrons. The expression for $\mu^\pm$, which was used to obtain the data of Fig. 6, is found to be

$$\mu^\pm=-\frac{1}{\epsilon}\left\{\sum_{N=0}^{\infty} N P_N^\pm \Big/ \ln\left[\sum_{N=0}^{\infty} P_N^\pm\left(\frac{\epsilon-1}{\epsilon}\right)^N\right]\right\}. \tag{10}$$

[23] C. D. Bowman, G. F. Auchampaugh, and S. C. Fultz, Lawrence Radiation Lab. (Livermore) Rept. UCRL-7468, 1963 (unpublished).

The error bars in Fig. 6 represent the standard deviation in μ due to the standard deviation in the P_N. These were computed by following the usual rules for propagation of error, through Eq. (10). The rather large error bars are due almost entirely to the low efficiency of the neutron detector. The factor $(1-1/\epsilon)$ of the denominator of Eq. (10) is always negative and, therefore, the sum terms in the denominator alternate in sign and increase the cumulative error. Because few high-multiplicity events are measured when the efficiency is small, the standard deviation is largest for these P_N. Since the largest errors are multiplied by large factors and the signs of the terms in the sum alternate, the relative errors in $\mu^{\pm}$ are quite large. The data could, of course, be greatly improved by increasing the efficiency of the detector. The energy dependence of $\mu^{\pm}$ given by the lines through the data of Fig. 6 was used in the subsequent analysis for μ.

The extraction of μ from the μ^+ and μ^- data is described elsewhere[23] in detail. With the assumption that the bremsstrahlung from positrons and electrons is identical, it is shown there that the required relation is

$$\mu=\mu^+\{1-[(\mu^+-\mu^-)/(\mu^+-\alpha\mu^-)]\}. \qquad (11)$$

In this expression α is the ratio of the total neutron yields measured with equal numbers of positrons and electrons and is obtained from Fig. 4 by dividing the upper curve by the lower curve. Equation (11) was used to compute μ as plotted in Fig. 7. The dashed lines represent the combined uncertainty of a 5% error in μ^+ and a 10% error in μ^-. These errors are rough estimates of the statistical uncertainty in the curves through the μ^+ and μ^- data. The data are fairly accurate up to 16 MeV. In the region above the giant resonance, μ is rather poorly determined since $\mu^+\approx\mu^-$ and α is near unity. A small uncertainty in the value of μ below 9 MeV arises since μ^+ was not measured in this region owing to insufficient positron intensity. However, when the electron energy is just slightly above threshold, only the high-energy tip of the bremsstrahlung spectrum may induce neutron emission. These photons are essentially monoenergetic so that near threshold $\mu^-=\mu$. The curve below 9 MeV was drawn so as to connect the value of μ near threshold, as determined by the value of μ^- at 7 MeV, to that at 9 MeV determined by μ^+ and μ^-.

There exists another means of treating the data to obtain the energy dependence of μ below the $(\gamma,2n)$ threshold. This procedure is independent of the determination by multiplicity measurements described above. Hopkins and Diven[15] have shown that the energy dependence of $\bar{\nu}$ is given by the relation

$$\bar{\nu}=A+0.160E\ (\text{MeV}), \qquad (12)$$

where the slope 0.160 MeV^{-1} is "universal" for neutron-induced fission of U^{233}, U^{235}, and Pu^{239}. This expression appears to hold accurately so long as the excitation

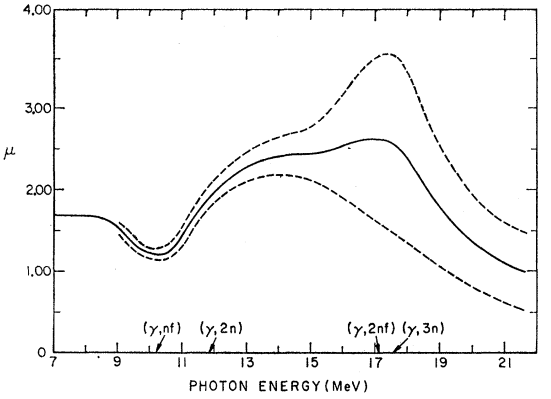

FIG. 7. The quantity μ as a function of photon energy. The solid curve was computed from the data of Fig. 6, using Eq. (11). The upper dashed line represents the value resulting when μ^+ and μ^- are, respectively, 5% and 10% higher than shown in Fig. 6. The lower dashed curve gives the value obtained when μ^+ and μ^- are lower in the same amount than the curves of Fig. 6.

energy exceeds the neutron-binding energy by about 2 MeV. On the assumption that this slope is a universal constant independent of the mode of nuclear excitation, Eq. (12) has been applied to the analysis for μ. Below the $(\gamma,2n)$ threshold, the expression for μ[Eq. (4)] can be written $\mu=\sigma(\gamma,N)/[\sigma(\gamma,N)-(\bar{\nu}-1)(\gamma,F)]$. Using the value of μ at 10 MeV obtained from the multiplicity experiment and the measured values of $\sigma(\gamma,F)$ and $\sigma(\gamma,N)$, $\bar{\nu}$ at 10 MeV can be determined. From Eq. (12), the value of A is 1.3. The energy dependence of $\bar{\nu}$ can, therefore, be established. The μ determined by this method falls within the error limits of the value obtained from the multiplicity determinations. The dip in μ at 10 MeV is therefore observed by two independent experiments. This fluctuation in μ is discussed in the next section.

INTERPRETATION

The dip in the μ curve would appear to indicate a variation in competition between neutron emission and fission in the decay of the compound nucleus. This competition can be expressed in terms of the ratio of widths for decay through either mode, Γ_n/Γ_f. This derives from the usual expression for partial cross sections in compound-nucleus reactions[24] $\sigma(\gamma,n)=\sigma(\gamma,\text{total})\Gamma_n/\Gamma$, which leads to the ratio $\sigma(\gamma,n)/\sigma(\gamma,f)=\Gamma_n/\Gamma_f$. This relation holds when the energy is below the $(\gamma,2n)$ and (γ,nf) thresholds if only fission and neutron emission are competing. With this restriction on energy, a simple expression for Γ_n/Γ_f can be derived from the definition of μ. Equation (4) gives $\Gamma_n/\Gamma_f=(\bar{\nu}-\mu)/(\mu-1)$. Using Eq. (12) for $\bar{\nu}$, Γ_n/Γ_f is found to increase from a value of 1.0 at 7 MeV to about 6 at 10 MeV. These numbers can be compared with

[24] J. M. Blatt and V. F. Weisskopf, *Theoretical Nuclear Physics* (John Wiley & Sons, Inc., New York, 1952).
[25] J. R. Huizenga, Phys. Rev. **109**, 484 (1958).

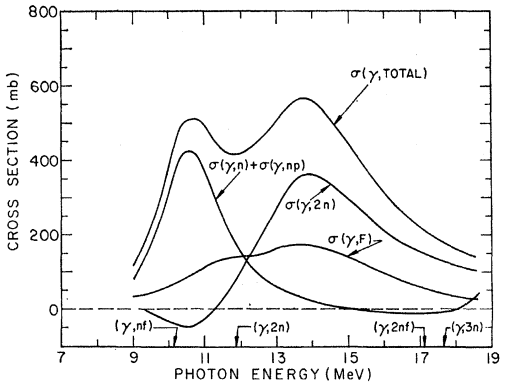

FIG. 8. The compound-nucleus-formation cross section $\sigma(\gamma,\text{total})$ and its components. The formation cross section was obtained by dividing $\sigma(\gamma,N)$ by μ. The (γ,n) and $(\gamma,2n)$ cross sections computed from Eqs. (14) are also shown. The (γ,F) cross section of Fig. 2 is included for comparison. The negative cross sections arise mainly from inaccuracies in the determination of μ and $\sigma(\gamma,F)$.

the bremsstrahlung weighted average of 1.6 obtained by Huizenga[25] from 12-MeV bremsstrahlung photofission-yield experiments.

The statistical model predicts that Γ_n/Γ_f should be independent of the nuclear-excitation energy. This was first shown by Fujimoto and Yamaguchi[26] who obtained the energy-independent expression

$$\Gamma_n/\Gamma_f=[TA^{2/3}/10]\exp[(E_f-B_n)/T]. \quad (13)$$

In this relation, (E_f-B_n) is the difference between the fission "threshold" and the neutron-binding energy and T is the nuclear temperature. Equation (13) was obtained by an extension of the Bohr–Wheeler[27] theory, using the constant-temperature approximation for the nuclear-level density, $\exp(E/T)$. Vandenbosch and Huizenga[28] have confirmed this correlation between Γ_n/Γ_f and the difference (E_f-B_n) for alpha-particle-induced fission and neutron emission. In an attempt to improve the calculation and perhaps obtain an explicit energy dependence, this relation was derived following the same procedure used by Fujimoto and Yamaguchi, but using the somewhat different dependence of the level density, $\exp(2(aE)^{1/2})$. The resulting expression is only very weakly dependent on the energy. Within the energy range $1<(E-E_f)<6$ MeV, Γ_n/Γ_f is found to change by less than 5%. Therefore, the decrease in μ near 9 MeV and the consequent large fluctuation in Γ_n/Γ_f probably cannot be explained by the use of more-accurate statistical expressions for nuclear-level density.

A clue regarding the mechanism responsible for the variation in Γ_n/Γ_f may lie in the observation that the ratio starts to increase as the photon energy reaches the realm of the giant dipole resonance. The photons in this energy region excite primarily positive-parity states in U^{235}. At lower energies where magnetic-dipole and electric-quadrupole interactions are predominant, negative-parity states are excited. This variation of Γ_n/Γ_f across the transition region of 8 to 10 MeV might, therefore, arise from the influence of parity either on the fissionability of the nucleus or on the level density of the residual nucleus following neutron emission.

The quantity Γ_n/Γ_f cannot be determined above 10 MeV in the straightforward manner described because the excitation energy exceeds the $(\gamma,2n)$ and/or (γ,nf) thresholds. However, the rise in μ above 10 MeV is expected since, between 10.2 and 11.8 MeV, the nucleus can boil off a neutron and be left in a state in which it must decay by fission if photon emission is neglected. The apparent decrease in μ above 18 MeV suggests the onset of the direct-interaction mechanism.

The measurements reported here also allow a unique determination of the compound-nucleus-formation cross section, neglecting photon scattering and charged-particle decay. From Eq. (4), it is clear that the formation cross section $\sigma(\gamma,\text{total})$ can be obtained by dividing the total neutron yield $\sigma(\gamma,N)$ by μ. The result is given in Fig. 8. The other curves of this figure show the component cross sections. The $\sigma(\gamma,F)$ curve was determined experimentally and the $\sigma(\gamma,n)$ and the $\sigma(\gamma,2n)$ were computed from the readily obtained relations

$$\begin{aligned}\sigma(\gamma,n)&=2\sigma(\gamma,\text{total})-\sigma(\gamma,N)+(\bar{\nu}-2)\sigma(\gamma,F),\\ \sigma(\gamma,2n)&=\sigma(\gamma,N)-\sigma(\gamma,\text{total})-(\bar{\nu}-1)\sigma(\gamma,F).\end{aligned} \quad (14)$$

These relations hold below the $(\gamma,3n)$ and $(\gamma,2nf)$ thresholds. The reappearance of the (γ,n) cross section near 18 MeV is perhaps indicative of the presence of direct interaction. However, it is equally likely to result from experimental uncertainties. A further indication of the uncertainties in the components is the appearance of the negative $(\gamma,2n)$ cross section below the $(\gamma,2n)$ threshold. Such aberrations are not unreasonable, considering the experimental uncertainties in the determination of μ and $\sigma(\gamma,F)$. The areas under these component curves between 9 and 18.5 MeV were found to be 1.07, 1.00, and 1.49 MeV·b for the $\sigma(\gamma,F)$, $\sigma(\gamma,n)$, and $\sigma(\gamma,2n)$ curves, respectively. The sum of these areas, 3.56 ± 0.43 MeV·b, corresponding to the integral of the formation cross section, is in good agreement with the value predicted by the Thomas–Reiche–Kuhn sum rule,

$$\int_0^\infty \sigma\ (\gamma,\text{total})\,dE=0.06\frac{NZ}{A}=3.36\ \text{MeV}\cdot\text{b}. \quad (15)$$

However, the measured value exceeds the sum rule by about 25% when wing corrections are included.

[26] Y. Fujimoto and Y. Yamaguchi, Progr. Theoret. Phys. (Kyoto) **5**, 76 (1950).
[27] N. Bohr and J. A. Wheeler, Phys. Rev. **56**, 426 (1939).
[28] R. Vandenbosch and J. R. Huizenga, in *Proceedings of the Second International Conference on the Peaceful Uses of Atomic Energy, Geneva, 1958* (United Nations, Geneva, 1958), Vol. 15, p. 284.

From Fig. 8, this area appears to be divided between two separate peaks. It is well-known that nuclei in this region of atomic weight are spheroidal in shape and, according to the hydrodynamical treatment by Danos and Okamoto, the giant dipole resonance should, therefore, be split into two components. The shape of each peak is defined by the dispersion formula

$$\sigma=\sigma_0/[1+(E^2-E_0^2)^2/\Gamma^2E^2], \quad (16)$$

where σ_0 is the peak cross section and Γ is the width of the resonance. For the prolate spheroid, the theory predicts the relation

$$\sigma_a\Gamma_a=\sigma_b\Gamma_b/2, \quad (17)$$

where the subscripts a and b denote the lower and upper energy peaks, respectively. The formation cross section has been analyzed, using Eq. (16) with the restriction imposed by Eq. (17). The $\sigma(\gamma,\text{total})$ curve of Fig. 8 was shape-fitted by use of an analog computer to obtain Γ and E_0 for the two resonances. For the lower-energy resonance, $\Gamma_a=2.45$ and $E_a=10.85$ MeV. The higher-energy resonance gave $\Gamma_b=4.00$ and $E_b=14.10$ MeV. The energies E_a and E_b can be used to predict the quadrupole moment, assuming a uniform charge distribution and a nuclear-charge radius for the nucleus. If the radius is taken to be $R=1.2\ A^{\frac{1}{3}}$ fermis, the resonance energies lead to a quadrupole moment of 12.8 ± 1.3 b. The error is based on a 2.5% uncertainty in the resonance energies. Deviations in the resonance energies larger than this clearly gave poorer fits to the cross-section curve. The sign is positive since the narrower peak occurs at the lower energy, indicating a prolate deformation. This value compares favorably with measurements of the quadrupole moment of 11.2 ± 0.6 and 9.0 ± 0.6 b obtained by Coulomb excitation[29] of the transitions between the ground-state and the 46.2- and 103-keV levels of U^{235}.

CONCLUSION

The measurements of the neutron yield and multiplicity with monochromatic photons of variable energy have made possible a determination of the compound-nucleus-formation cross section of U^{235} which properly takes into account any variation in competition between neutron emission and fission. The resulting integrated cross section is in fair agreement with theory. A splitting in the resonance has been observed and Lorentz curves fitted to obtain the intrinsic quadrupole moment of the nucleus. The value is in good agreement with that found by Coulomb excitation. These measurements were complemented by the determination of the photofission cross section of U^{235}. With this additional information, it was possible to determine the (γ,n) and $(\gamma,2n)$ cross sections as well. In addition, a rather strong energy dependence in Γ_n/Γ_f on the lower side of the giant dipole resonance was observed. It is pointed out that this anomalous behavior is possibly a consequence of the parity of the compound nucleus.

ACKNOWLEDGMENTS

The authors wish to acknowledge the many enlightening conversations with Dr. Richard L. Bramblett, the assistance of Dr. Donald Davis in the development of the statistical analysis, and the helpful cooperation of the Linac operating crew. The work was done under the auspices of the U. S. Atomic Energy Commission.

[29] J. O. Newton, Nucl. Phys. 5, 218 (1958).